# Unsupervised Change Detection in Optical Satellite Images using Binary Descriptor

Neha Gupta, Gargi V. Pillai, Samit Ari
Department of Electronics and Communication Engineering,
National Institute of Technology, Rourkela, India 769008.
Email: neha27brs@gmail.com, gargipillai92@gmail.com, samit@nitrkl.ac.in

***Abstract*—In this paper, a novel unsupervised technique is proposed to get the change analysis of multitemporal satellite images. The proposed technique is based on the local binary similarity pattern (LBSP) concept. In this binary descriptor, inter-LBSP is used to detect the changes. In this approach, the main challenge is to calculate the threshold which is used to generate the binary feature vectors. Here, an effective solution has been found, where the neighbourhood information is used for calculation of threshold. Both images are partitioned into overlapping image blocks which are used to calculate the threshold. This calculated threshold is used to obtain binary feature vectors for each pixel of both images. To get the binary feature vectors, difference between neighbouring pixels and center pixel of each block is compared with the calculated threshold. Hamming distance is used as a similarity metric to compare the binary vectors of each image for each pixel position which gives the binary change map of changed and unchanged region. To obtain this binary change map, calculated hamming distance is compared with empirically chosen minimum similarity value. Optical satellite images acquired by Landsat satellite are used to perform the experiments. Experimental results show that the proposed method provides better results compared to earlier reported techniques like expectation maximization and kernel $k$-means methods.**

***Index Terms*—Change detection, multitemporal satellite image, local binary similarity pattern (LBSP), binary change map.**

## I. Introduction

Remote sensing is the process to observe or perceive any object from a distance without direct contact with that object. Remote sensors like satellites or airborne sensors are collecting data by detecting the energy reflected from Earth. Change detection, orthorectification, spectral analysis and image classification are the applications of the remote sensing. The main focus of this paper is to examine the change detection which is one of the above–mentioned applications of remote sensing. Change detection is the procedure to distinguish differences in an object or phenomenon by observing it at various times [1].

Change detection is useful in many applications such as land-use change, deforestation, forest fire, landscape change, forest or vegetation change, urban change, wetland change, environmental change [2].

In the reported literature [1]–[3], two types of approaches are mainly used to detect the changes in multitemporal satellite images: 1) supervised [4]–[6] and 2) unsupervised approaches [7]–[12]. The former approach is based on the use of supervised classifiers which requires ground truth information. This ground truth information can be acquired with field campaigns or from prior knowledge on the area which require time and effort. On the contrary, there is no need of any ground truth data for change detection technique in unsupervised approach and thus it is mainly used for change detection application [3].

Many reported unsupervised methods analyse difference image that are obtained by taking the difference of images acquired at two times. In [13], the difference image is analysed with two automatic approach based on the Bayes theory. First approach assumed that pixels are independent to each other and gives an automatic selection of a decision threshold value which will separate the changed and no-changed pixels. Second approach has considered the contextual information based on Markov random fields theory that exploits interpixel dependency. Statistical terms are estimated with an iterative method expectation–maximization (EM) algorithm. In [9], difference image is analyzed in two stages: In the first stage, features are extracted with principal component analysis (PCA) and in second stage, obtained features for each pixel are clustered with k-means clustering algorithm. Partitioned image is used to create the eigen vector space using PCA then this eigen vector space is used to extract the feature around each pixel. To get two clusters change and no change, k-means clustering is applied on obtained feature vector around each pixel. In [14], again the difference image is analyzed in two stages: feature extraction and k-means clustering. Multiscale features are extracted by subbands decomposition of undecimated discrete wavelet transform (UDWT). These multiscale feature vectors for each pixel are further clustered in two classes using k-means clustering algorithm. In [15], the difference image is analyzed in original domain and also in kernel domain using the nonlinear transformation approach based on kernels. Here, the kernel k-means (KKM) algorithm is applied to partition the image into two classes change and no change. In [16], multitemporal images are anayzed separately to obtain the binary descriptor for each pixel. Comparison of these descriptors are done using XOR operation. Hamming distance is calculated for each pixel for clustering the pixels. Binary change map is generated by applying the Lloyd−Max's algorithm to obtain hamming distance for each pixel.

Binary descriptors are very discriminative, fast and robust to noise. Most of binary descriptors are based on evaluating many comparisons of pixels intensity in different combinations. Large number of binary comparisons make it robust to noise [17]. Motivated by this, local binary similarity patterns (LBSP) based method is proposed in this paper [18]. As the LBSP can be calculated for two regions inside same image or across region between two images to detect the differences with respect to intensity. Proposed method analyses the multitemporal images to obtain the binary change map. Here, across region between two images are taken to calculate the binary vectors. Unlike the conventional LBSP threshold calculation , in proposed method binary vector is created with help of threshold calculated in a different way. The similarity between the binary feature vectors for each pixel is measured with hamming distance to get binary change map.

This paper is organized as follows: Sections II explains the proposed method for unsupervised change detection. Experimental results with database description, qualitative and quantitative assessment are presented in Sections III. Section IV concludes this paper.

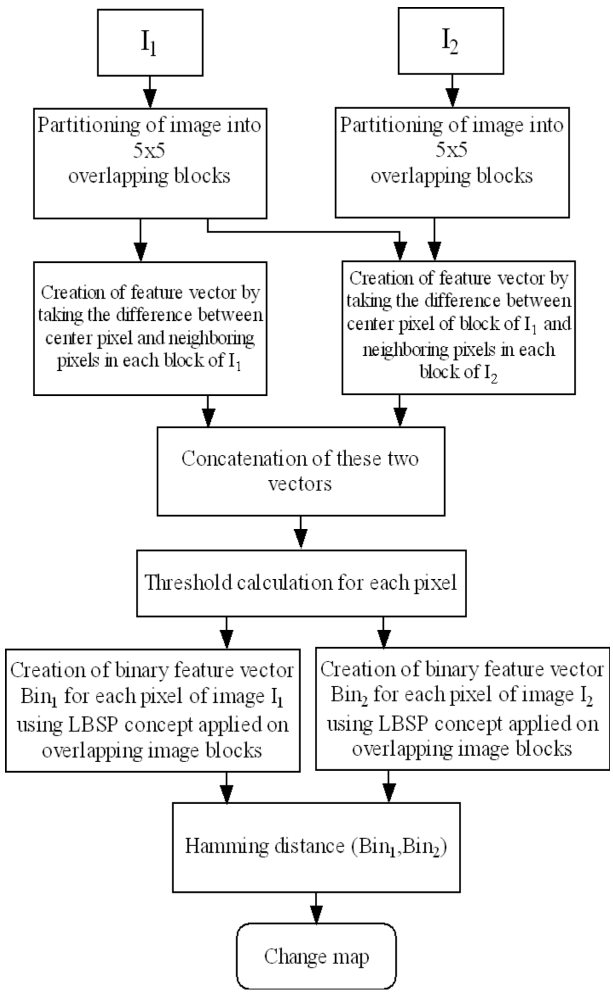


Fig. 1. Block diagram of the proposed approach.

## II. Proposed Method

Two coregistered images $I_1$ and $I_2$ with size $m \times n$ of the same geographical region taken at two different times are considered. The main challenge is to obtain the binary change detection map with change and no change information of a geographical region occurred within a time duration. The block diagram of the proposed approach is shown in Fig. 1. The proposed approach consists two parts: threshold calculation and generation of binary map.

The proposed approach is described as follows:

### A. Partitioning of images into overlapping blocks

In this stage, two multitemporal satellite images $I_1$ and $I_2$ are taken. Each image is partitioned into $5 \times 5$ overlapping blocks. For each pixel of the image there is a block of $5 \times 5$ size and every pixel is the center pixel of each block. Here, the image $I_1$ is taken as reference image.

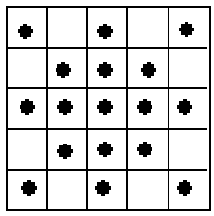

Fig. 2. Representation of number of elements used in $5 \times 5$ block.

### B. Creation of feature vectors

According to the LBSP concept [18], from the $5 \times 5$ block only 16 elements are considered. In this paper, 17 elements including the center pixel are represented in Fig. 2. The image $I_1$ is taken as the reference image therefore center pixel of the image $I_1$ is considered for the analysis.

Now two difference vectors are created for each pixel position. First vector is created by taking absolute difference between center pixel and neighbouring pixels of block of image $I_1$. Second vector is created by taking absolute difference between center pixel of block of reference image $I_1$ and neighbouring pixels of block of image $I_2$. The size of both vectors is $16 \times 1$. These vectors are represented as follows:

$$Diff_1\,(d,c) = \{x_1, x_2, \cdots, x_{16}\} \tag{1}$$

$$Diff_2\,(d,c) = \{y_1, y_2, \cdots, y_{16}\} \tag{2}$$

where $Diff_1$ represents the difference vector created by neighbouring pixels and center pixel of blocks of reference image and $Diff_2$ represents the difference vector created by center pixel of blocks of reference image and neighbouring pixels of blocks of other image. $(d, c)$ represents the position of the pixel in image where $d = \{1, 2, \cdots, m\}$ and $c = \{1, 2, \cdots, n\}$.

### C. Concatenation of feature vectors

Both obtained feature vectors for each position is concatenated to get the vector of size $32 \times 1$ which is represented by $Diff$.

$$Diff_{(d,c)} = \{Diff_1\,(d,c)\,, Diff_2\,(d,c)\} \tag{3}$$

$$Diff_{(d,c)} = \{x_1, x_2, \cdots, x_{16}, y_1, y_2, \cdots, y_{16}\} \tag{4}$$

### D. Threshold calculation

Threshold is calculated by taking the mean of above obtained vector. Corresponding blocks of both images are considered to calculate threshold values for each pixel which will result in vector of size $N \times 1$, where the number of pixels in a single image is represented as $N$ i.e. $m \times n$.

$$th(d,c) = \frac{1}{M} \sum_{k=1}^{32} Diff_{(d,c)}(k) \tag{5}$$

where the number of non zero elements in vector $Diff$ is represented as $M$.

### E. Creation of binary feature vectors

Calculated threshold from the first part of the proposed method is used to generate the binary feature vector for each pixel in this section. Here, again $5 \times 5$ overlapping blocks of each image is taken as in the previous part of the proposed method.

Using the LBSP concept, binary feature vector for each pixel of each image is created using above calculated threshold. Therefore, two binary feature vectors are created for each pixel position. First binary vector is created by taking the absolute difference between center pixel and neighbouring pixels of block of image $I_1$ and assigning '0' or '1' according to calculated threshold. Second binary vector is created by taking absolute difference between center pixel of block of reference image $I_1$ and neighbouring pixels of block of image $I_2$ and assigning '0' or '1' according to calculated threshold.

These are calculated using following equations,

$$Bin_1(d,c) = \begin{cases} 1, & \text{if } |Ne_1(P) - C_1(d,c)| > th(d,c) \\ 0, & \text{else} \end{cases} \tag{6}$$

$$Bin_2(d,c) = \begin{cases} 1, & \text{if } |Ne_2(P) - C_1(d,c)| > th(d,c) \\ 0, & \text{else} \end{cases} \tag{7}$$

where, $Bin_1$ and $Bin_2$ represent the binary feature vector for each pixel of reference image and other image respectively. $Ne_1$ and $Ne_2$ are the neighbouring pixels in blocks of the reference image and other image respectively. $P$ represents the number of neighbouring pixels in that block. $C_1$ is the center of blocks of reference image.

A $16 \times 1$ size binary feature vector is obtained for each pixel of reference image and other image.

### F. Hamming distance calculation

Hamming distance is used to compare the binary feature vectors of each image. Hamming distance can be performed mathematically with XOR operation and a counter. Hamming distance is calculated in terms of the counter which gives the number of ones present in the XOR output.

XOR operation is performed to compare the binary vectors for each pixel. A counter is applied on vector obtained by XOR operation to get the maximum similarity.

$$out_{xor}(d,c) = Bin_1(d,c) \oplus Bin_2(d,c) \tag{8}$$

where $out_{xor}$ is the output of XOR operation.

$$out_{(d,c)}(q) = \sum_{k=1}^{16} [out_{xor}(d,c) = q] \tag{9}$$

where [ ] is the Iverson bracket and $q$ represent the 1 presented in XOR output and $out$ is counter output for each pixel.

### G. Binary Change Map

The binary change map is created on the basis of maximum similarity of corresponding pixel in each image. If for any pixel, the hamming distance is giving the maximum similarity between two binary feature vectors of the corresponding pixel position then that pixel will be considered as unchanged pixel.

Generation of the binary change map is represented as follows:

$$cm(d,c) = \begin{cases} 1, & \text{if } out_{(d,c)}(q) < \text{ minimum similarity} \\ 0, & \text{else} \end{cases} \tag{10}$$

where '1' represents the unchanged region and '0' represents the changed region. Here, the minimum similarity means the similarity between the two binary feature vector of both images at same pixel position is minimum. If the number of '1' exceeds a minimum value in output of the counter, then the corresponding pixel will be classified as changed pixel.

## III. Experimental Results

The performance of the proposed approach is tested in real data sets. Landsat satellite images are considered to perform the experiments.

### A. Database Description

Dataset I: The dataset is acquired by Landsat 5 Thematic Mapper (TM) sensor on May 29, 2009, and November 09, 2011 [19]. The study area is an upper lake of the Bhopal city situated in Madhya Pradesh, India having size of $206 \times 424$ pixels. The lake is dried in 2009 because of the insufficient rains. The pair of multitemporal images of dataset are shown in Fig. 3.(a) and (b). The reference map or ground truth which is shown in Fig. 3.(c), represents the change and no change information. It is created manually by detailed visual analysis of input images captured at two different times.

Dataset II: This dataset consists of two images acquired at different times by Landsat 7 Enhanced Thematic Mapper Plus (ETM+) Sensor on February 09, 2001 and September 21, 2001 [19]. The study area is Natural Lake, situated in Jaisalmer district, Rajasthan, India. The main change is that this lake was also dried in summer. The size of the image used for the experiment is $220 \times 550$ pixels shown in Fig. 4.(a) and (b). The reference map or ground truth which is shown in Fig. 4.(c), represents the change and no change information. It is created manually by detailed visual analysis of input images captured at two different times.

### B. Qualitative Results

To get the rough idea about the generated binary change detection map visual results are given in qualitative assessment. Here, the visual results are compared with the ground truth. Black pixels are showing the change region and white pixels are showing the unchanged region in generated binary map. The proposed method is compared with earlier reported technique like EM [13] and KKM [15] method. The visual binary change maps of EM [13], KKM [15] and proposed methods are shown in Fig. 3(d), (e), and (f) receptively for dataset I. Fig. 4(d), (e), and (f) show the visual binary change maps of EM [13], KKM [15] and proposed methods respectively for dataset II. Results shows that the proposed method is better than EM [13] and KKM [15] methods. From the visual results, it can be observed that even the small changes are being detected by the proposed method.

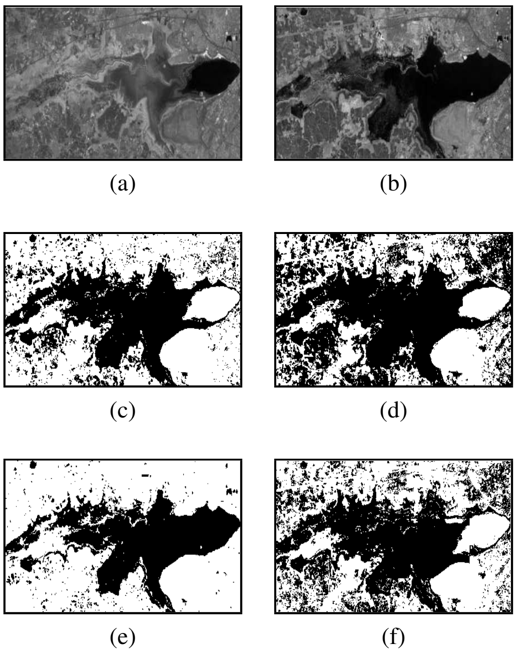


Fig. 3. Optical satellite data used for the experiment and visual results on dataset obtained by comparing methods and proposed methods. (a) and (b) are Landsat 5 TM (band 4) multitemporal images of Bhopal city. (c) is ground truth. (d), (e) and (f) are visual results by EM [13], KKM [15], and proposed approaches respectively.

### C. Quantitative Results

In qualitative results, generated change map using proposed method is compared with EM [13] and KKM [15] methods with respect to some predefined parameters [20], [21]. The quantitative measures are defined as follows: 1) Correct classification or overall accuracy in percentage: $(P_{CC} = ((TP + TN)/(N_0 + N_1) \times 100))$, where true positives ($TP$) are the number of "changed" pixels that are correctly detected and true negatives ($TN$) are the number of "unchanged" pixels that are correctly detected, 2) False positives ($FP$): the number of "unchanged" pixels that are incorrectly detected as "changed" (also known as false alarms), and $P_{FP} = FP/(N_1)$. 3) Total error in percentage: $(P_{TE} = ((FP + FN)/(N0 + N1)) \times 100)$, where false negatives ($FN$) are the number of "changed" pixels that are incorrectly detected as "unchanged". $N_1$ and $N_0$ are the total number of unchanged and changed pixels in the ground truth respectively. 4) Kappa coefficient [22], a robust measure is also adopted which compares an observed accuracy with an expected accuracy (random chance).

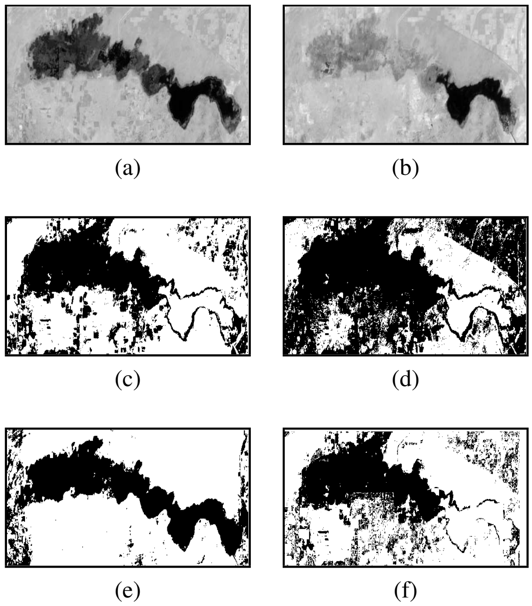


Fig. 4. Optical satellite data used for the experiment and visual results on dataset obtained by comparing methods and proposed methods. (a) and (b) are Landsat 7 ETM+ (band 4) multitemporal images respectively of Bhopal city. (c) is ground truth. (d), (e) and (f) are visual results by EM [13], KKM [15], and proposed approaches respectively.

Expectation maximization and kernel $k$-means methods are implemented with default parameters given in [13] and [15] respectively. The results with quantitative measures is shown in Table 1. The value of the minimum similarity is determined experimentally that is giving the lowest error rate or maximum accuracy. In this experiment, this value is chosen empirically as 8. As shown in the table, the proposed method achieves 85.71% accuracy and 14.29% total error for dataset I. For dataset II, the proposed method achieves 85.99% accuracy which is better than the compared methods. The proposed method provides 68.70% and 79.03% kappa values for datasets I and II respectively which are better than the compared methods. The false alarm rate which shows the number of unchanged pixels getting as changed is better than the EM [13] and KKM [15] methods in both datasets.

## IV. Conclusion

In this paper, an unsupervised LBSP based technique is proposed. Neighbourhood information along with the center pixel is used to calculate the threshold. Since the local information is used to calculate the threshold for each block, this results in better performance. Binary vector is evaluated using LBSP concept with the calculated threshold for each pixel of both images. Hamming distance

Table I
QUANTITATIVE MEASURES(IN PERCENTAGE)

| Dataset | Change Detection Method | $P_{CC}$ | $P_{FA}$ | $P_{TE}$ | $\kappa$ |
|---|---|---|---|---|---|
| Bhopal City | EM [13] | 82.82 | 27.74 | 17.18 | 66.48 |
| | KKM [15] | 84.64 | 7.46 | 15.36 | 66.38 |
| | Proposed | 85.71 | 6.44 | 14.29 | 68.70 |
| Natural Lake | EM [13] | 74.86 | 38.45 | 25.14 | 52.57 |
| | KKM [15] | 75.19 | 15.07 | 24.81 | 43.24 |
| | Proposed | 85.99 | 3.38 | 14.01 | 79.03 |

is used as a similarity metric to compare corresponding pixel of both images to detect it as a change or no change. To compare the hamming distance, minimum similarity is chosen empirically in proposed method. Experiment performed on real optical satellite images shows the effectiveness of proposed descriptor based approach over difference image based approaches such as EM and KKM. Qualitative results show that the proposed technique detects big changes as well as small changes with less false alarms. The proposed method yields better accuracy and higher kappa value compared to earlier reported approaches.

## REFERENCES


[1] A. Singh, "Review article digital change detection techniques using remotely-sensed data," *Int. J. Remote Sens.*, vol. 10, no. 6, pp. 989–1003, 1989.

[2] D. Lu, P. Mausel, E. Brondizio, and E. Moran, "Change detection techniques," *Int. J. Remote Sens.*, vol. 25, no. 12, pp. 2365–2401, 2004.

[3] L. Bruzzone and F. Bovolo, "A novel framework for the design of change-detection systems for very-high-resolution remote sensing images," *Proceedings of the IEEE*, vol. 101, no. 3, pp. 609–630, 2013.

[4] L. Bruzzone and S. B. Serpico, "An iterative technique for the detection of land-cover transitions in multitemporal remote-sensing images," *IEEE Trans. Geosci. Remote Sens.*, vol. 35, no. 4, pp. 858–867, 1997.

[5] L. Bruzzone, R. Cossu, and G. Vernazza, "Detection of land-cover transitions by combining multidate classifiers," *Pattern Recognit. Lett.*, vol. 25, no. 13, pp. 1491–1500, 2004.

[6] L. Bruzzone and R. Cossu, "A multiple-cascade-classifier system for a robust and partially unsupervised updating of land-cover maps," *IEEE Trans. Geosci. Remote Sens.*, vol. 40, no. 9, pp. 1984–1996, 2002.

[7] F. Bovolo and L. Bruzzone, "A theoretical framework for unsupervised change detection based on change vector analysis in the polar domain," *IEEE Trans. Geosci. Remote Sens.*, vol. 45, no. 1, pp. 218–236, 2007.

[8] L. Bruzzone and D. F. Prieto, "An adaptive parcel-based technique for unsupervised change detection," *Int. J. Remote Sens.*, vol. 21, no. 4, pp. 817–822, 2000.

[9] T. Celik, "Unsupervised change detection in satellite images using principal component analysis and-means clustering," *IEEE Geosci. Remote Sens. Lett.*, vol. 6, no. 4, pp. 772–776, 2009.

[10] G. Moser, E. Angiati, and S. B. Serpico, "Multiscale unsupervised change detection on optical images by markov random fields and wavelets," *IEEE Geosci. Remote Sens. Lett.*, vol. 8, no. 4, pp. 725–729, 2011.

[11] M. N. Sumaiya and R. S. S. Kumari, "Logarithmic mean-based thresholding for sar image change detection," *IEEE Geosci. Remote Sens. Lett.*, vol. 13, no. 11, pp. 1726–1728, Nov 2016.

[12] L. Jia, M. Li, P. Zhang, Y. Wu, and H. Zhu, "Sar image change detection based on multiple kernel k-means clustering with local-neighborhood information," *IEEE Geosci. Remote Sens. Lett.*, vol. 13, no. 6, pp. 856–860, 2016.

[13] L. Bruzzone and D. F. Prieto, "Automatic analysis of the difference image for unsupervised change detection," *IEEE Trans. Geosci. Remote Sens.*, vol. 38, no. 3, pp. 1171–1182, 2000.

[14] T. Celik, "Multiscale change detection in multitemporal satellite images," *IEEE Geosci. Remote Sens. Lett.*, vol. 6, no. 4, pp. 820–824, 2009.

[15] M. Volpi, D. Tuia, G. Camps-Valls, and M. Kanevski, "Unsupervised change detection with kernels," *IEEE Geosci. Remote Sens. Lett.*, vol. 9, no. 6, pp. 1026–1030, 2012.

[16] A. Radoi and M. Datcu, "Automatic change analysis in satellite images using binary descriptors and lloyd–max quantization," *IEEE Geosci. Remote Sens. Lett.*, vol. 12, no. 6, pp. 1223–1227, 2015.

[17] G.-A. Bilodeau, J.-P. Jodoin, and N. Saunier, "Change detection in feature space using local binary similarity patterns," in *Computer and Robot Vision (CRV), 2013 International Conference on*. IEEE, 2013, pp. 106–112.

[18] P.-L. St-Charles, G.-A. Bilodeau, and R. Bergevin, "Subsense: A universal change detection method with local adaptive sensitivity," *IEEE Trans. Image Process.*, vol. 24, no. 1, pp. 359–373, 2015.

[19] [Online]. Available: http://earthexplorer.usgs.gov/

[20] T. Celik, "Image change detection using gaussian mixture model and genetic algorithm," *J. Vis. Commun. Image Represent.*, vol. 21, no. 8, pp. 965–974, 2010.

[21] H.-C. Li, T. Celik, N. Longbotham, and W. J. Emery, "Gabor feature based unsupervised change detection of multitemporal sar images based on two-level clustering," *IEEE Geosci. Remote Sens. Lett.*, vol. 12, no. 12, pp. 2458–2462, 2015.

[22] G. M. Foody and A. Mathur, "A relative evaluation of multiclass image classification by support vector machines," *IEEE Trans. Geosci. Remote Sens.*, vol. 42, no. 6, pp. 1335–1343, 2004.